Eur. Phys. J. A 18, 231–235 (2003)
DOI 10.1140/epja/i2002-10206-6

THE EUROPEAN PHYSICAL JOURNAL A

Facets of confinement and dynamical chiral symmetry breaking

P. Maris[1], A. Raya[2], C.D. Roberts[3,4,a], and S.M. Schmidt[5]

[1] Department of Physics, North Carolina State University, Raleigh NC 27695-8202, USA
[2] Instituto de Física y Matemáticas, Universidad Michoacana de San Nicolás de Hidalgo, Apartado Postal 2-82, Morelia, Michoacán, México
[3] Physics Division, Argonne National Laboratory, Argonne IL 60439-4843, USA
[4] Fachbereich Physik, Universität Rostock, D-18051 Rostock, Germany
[5] Helmholtz-Gemeinschaft, Ahrstrasse 45, D-53175 Bonn, Germany

Received: 30 September 2002 /
Published online: 22 October 2003 –

Abstract. The gap equation is a cornerstone in understanding dynamical chiral symmetry breaking and may also provide clues to confinement. A symmetry-preserving truncation of its kernel enables proofs of important results and the development of an efficacious phenomenology. We describe a model of the kernel that yields: a momentum-dependent dressed-quark propagator in fair agreement with quenched lattice-QCD results; and chiral limit values, $f_\pi^0 = 68\,\mathrm{MeV}$ and $\langle \bar{q}q \rangle = -(190\,\mathrm{MeV})^3$. It is compared with models inferred from studies of the gauge sector.

PACS. 12.38.Aw General properties of QCD (dynamics, confinement, etc.) – 11.30.Rd Chiral symmetries

1 Introduction

We will address these topics from the perspective of QCD's Dyson-Schwinger equations (DSEs) [1]. The DSEs are a keystone in proving renormalisability and provide a generating tool for perturbation theory. The latter point is very important in applications to low-energy phenomena because it means that the model-dependence which necessarily appears in continuum studies of nonperturbative QCD is restricted to the infrared; *i.e.*, to momentum scales $\lesssim 1\,\mathrm{GeV}^2$. This feature has successfully been exploited in applications to the spectra [2,3], and strong [4] and electroweak [5] interactions of mesons. It also mitigates, to a useful extent, some of the problems with the approach; *e.g.*, it helps in developing reliable truncations for the coupled system of DSEs.

Recent successes are founded on an accurate understanding of dynamical chiral symmetry breaking (DCSB), and its role in resolving the dichotomy of the pion [6] (as both a Goldstone mode and a massless bound state of massive constituents) and its relation to the long-range behaviour of the effective coupling between quarks [7].

[a] e-mail: cdroberts@anl.gov

2 Dynamical chiral symmetry breaking

This is a purely nonperturbative phenomenon that can be studied via QCD's gap equation:

$$S(p)^{-1} = (i\gamma\cdot p + m) + \int \frac{\mathrm{d}^4 q}{(2\pi)^4}\, g^2 D_{\mu\nu}(p-q)\frac{\lambda^a}{2}\gamma_\mu S(q)\Gamma^a_\nu(q,p)\,, \tag{1}$$

wherein m is the current-quark bare mass, g is the coupling constant, $D_{\mu\nu}(p-q)$ is the dressed-gluon propagator, $\Gamma^a_\nu(q,p)$ is the dressed-quark-gluon vertex; and the solution is the dressed-quark propagator

$$S(p) = \frac{1}{i\gamma\cdot p\, A(p^2) + B(p^2)} = \frac{Z(p^2)}{i\gamma\cdot p + M(p^2)}\,. \tag{2}$$

(Equation (1) is the unrenormalised equation: renormalisation will only be mentioned as necessary.)

As noted in the introduction, one can use the gap equation to evaluate the fermion self-energy perturbatively and thereby obtain

$$B(p^2) = m\left(1 - \frac{\alpha}{\pi}\ln\left[\frac{p^2}{m^2}\right] + \ldots\right)\,, \tag{3}$$

wherein the ellipsis denotes two- and higher-loop contributions. It is apparent that each term is proportional to the current-quark mass and vanishes as $m \to 0$. Hence, in perturbation theory, if there is no quark mass to begin with, interactions do not generate one; *i.e.*, DCSB is impossible in perturbation theory.

In the chiral limit, namely, $m = 0$, eq. (1) always admits the trivial solution $B(p^2) \equiv 0$; *i.e.*, the solution accessible perturbatively. However, as is characteristic of gap equations, when the integrated strength of the kernel exceeds some critical value, a $B(p^2) \neq 0$ solution is generated. This nonperturbative, dynamical generation of a quark mass *from nothing* is DCSB. The integrated strength of the kernel can be characterised by an interaction tension, σ^{Δ}, for which the critical value is [8] $\sigma^{\Delta}_{\mathrm{c}} \sim 2.5\,\mathrm{GeV/fm}$: this strength provides for DCSB *but only just*. An acceptable description of hadrons requires [2] $\sigma^{\Delta} \sim 25\,\mathrm{GeV/fm}$, which is an order of magnitude larger.

2.1 Symmetry-preserving truncation

It is apparent that the gap equation's kernel is formed from a product of the dressed-gluon propagator and dressed-quark-gluon vertex. It may be calculated in perturbation theory but that is inadequate for the study of intrinsically nonperturbative phenomena. Consequently, to make sensible statements about DCSB, one must employ an alternative systematic and chiral symmetry-preserving truncation scheme.

One must also focus on more than just the gap equation's kernel. Chiral symmetry is expressed via the axial-vector Ward-Takahashi identity:

$$P_\mu\, \Gamma_{5\mu}(k;P) = S^{-1}(k_+)\, i\gamma_5 + i\gamma_5\, S^{-1}(k_-)\,, \tag{4}$$

$k_\pm = k \pm P/2$, wherein $\Gamma_{5\mu}(k;P)$ is the dressed axial-vector vertex. This three-point function satisfies an inhomogeneous Bethe-Salpeter equation:

$$\begin{aligned}[\Gamma_{5\mu}(k;P)]_{tu} &= [\gamma_5\gamma_\mu]_{tu} \\ &+ \int \frac{\mathrm{d}^4 q}{(2\pi)^4} [S(q_+)\Gamma_{5\mu}(q;P)S(q_-)]_{sr} K^{rs}_{tu}(q,k;P)\,,\end{aligned} \tag{5}$$

in which $K(q,k;P)$ is the fully amputated quark-antiquark scattering kernel. The Ward-Takahashi identity, eq. (4), means that the kernel in the gap equation and that in the Bethe-Salpeter equation are intimately related. Therefore, a qualitatively reliable understanding of chiral symmetry and its dynamical breaking can only be obtained using a truncation scheme that preserves this relation, and hence guarantees eq. (4) without a *fine-tuning* of model-dependent parameters.

One such scheme exists [9]. Its leading-order term is the renormalisation-group-improved rainbow-ladder truncation and the general procedure provides a means to identify, *a priori*, those channels in which that truncation is likely to be accurate. This scheme underlies the successful application of a rainbow-ladder model to flavour-nonsinglet pseudoscalar mesons and vector mesons [2–5]. The systematic nature of the scheme has also made possible a proof of Goldstone's theorem in QCD [6] and the derivation of a mass formula that unifies the light- and heavy-quark sectors [10].

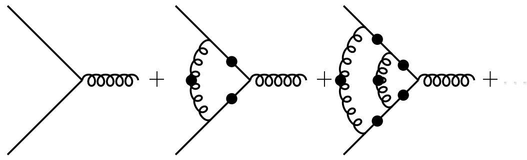

Fig. 1. Planar dressed-quark-gluon vertex obtained by neglecting contributions associated with explicit gluon self-interactions. The solid circles indicate fully dressed propagators. The quark-gluon vertices are not dressed.

Table 1. π- and ρ-meson masses obtained with $\mathcal{G} = 0.48\,\mathrm{GeV}$. (Dimensioned quantities in GeV.) n is the number of dressed-gluon rungs retained in the planar vertex, see fig. 1, and hence the order of the vertex-consistent Bethe-Salpeter kernel.

	$M_H^{n=0}$	$M_H^{n=1}$	$M_H^{n=2}$	$M_H^{n=\infty}$
π, $m = 0$	0	0	0	0
π, $m = 0.011$	0.152	0.152	0.152	0.152
ρ, $m = 0$	0.678	0.745	0.754	0.754
ρ, $m = 0.011$	0.695	0.762	0.770	0.770

In this scheme, as in perturbation theory, it is impossible, in general, to obtain complete closed-form expressions for the kernels of the gap and Bethe-Salpeter equations. However, for the planar dressed-quark-gluon vertex depicted in fig. 1, closed forms can be obtained and a number of significant features illustrated [11] when one uses the following model for the dressed-gluon line [12]:

$$g^2 D_{\mu\nu}(k) = \left[\delta_{\mu\nu} - \frac{k_\mu k_\nu}{k^2}\right] (2\pi)^4\, \mathcal{G}^2\, \delta^4(k)\,, \tag{6}$$

where $\mathcal{G}$, measured in GeV, sets the model's mass-scale. This form is a precursor to the class of renormalisation-group-improved models. It has many positive features in common with that class and, furthermore, its particular momentum-dependence works to advantage in reducing integral equations to character-preserving algebraic equations. Naturally, there is a drawback: the simple momentum dependence also leads to some model-dependent artefacts, but they are easily identified and hence not cause for concern.

It is a general result [11] that with any vertex whose diagrammatic content is known explicitly; *e.g.*, fig. 1, it is always possible to construct a unique Bethe-Salpeter kernel which ensures the Ward-Takahashi identities are automatically fulfilled: that kernel is necessarily non-planar. This becomes transparent with the model in eq. (6), using which the gap equation obtained with the vertex depicted in fig. 1 reduces to an algebraic equation, irrespective of the number of dressed-gluon rungs that are retained, and the same is true of the Bethe-Salpeter equations in every channel: pseudoscalar, vector, etc.

Results for the π and ρ are illustrated in table 1. It is evident that, irrespective of the order of the truncation; *i.e.*, the value of n, the number of dressed gluon rungs in the quark-gluon vertex, the pion is massless in the chiral limit. (N.B. This pion is composed of heavy dressed quarks, as is evident in the calculated scale of the dynamically generated dressed-quark mass function: $M(0) \approx 0.5\,\text{GeV}$.) The masslessness of the π is a model-independent consequence of the consistency between the Bethe-Salpeter kernel and the kernel in the gap equation. Furthermore, the bulk of the ρ-π mass splitting is present in the chiral limit and with the simplest ($n = 0$; *i.e.*, rainbow-ladder) kernel, which makes plain that this mass difference is driven by the DCSB mechanism: it is not the result of a finely adjusted hyperfine interaction. Finally, the quantitative effect of improving on the rainbow-ladder truncation; *i.e.*, including more dressed-gluon rungs in the gap equation's kernel and consistently improving the kernel in the Bethe-Salpeter kernel, is a 10% correction to the vector meson mass. Simply including the first correction ($n = 1$, *i.e.*, retaining the first two diagrams in fig. 1) yields a vector meson mass that differs from the fully resummed result by $\lesssim 1\%$. The rainbow-ladder truncation is clearly accurate in these channels.

2.2 Rainbow-ladder truncation

The renormalisation-group-improved rainbow-ladder truncation is based on the fact that in QCD, on the domain for which $Q^2 := (k-q)^2 \sim k^2 \sim q^2$ is large and spacelike,

$$\begin{aligned} M(q,k;P) &:= g^2(\mu^2)\, D_{\mu\nu}(k-q) \\ &\quad \times \left[\Gamma^a_\mu(k_+,q_+) S(q_+)\right] \otimes \left[S(q_-)\, \Gamma^a_\nu(q_-,k_-)\right] \\ &= 4\pi\, \alpha(Q^2)\, D^{\text{free}}_{\mu\nu}(k-q) \\ &\quad \times \left[\frac{\lambda^a}{2}\gamma_\mu\, S^{\text{free}}(q_+)\right] \otimes \left[S^{\text{free}}(q_-)\,\frac{\lambda^a}{2}\gamma_\nu\right], \end{aligned} \tag{7}$$

where $\alpha(Q^2)$ is the strong running coupling and, *e.g.*, S^{free} is the free quark propagator. The dressed-ladder truncation supposes that eq. (7) is valid for all momenta and is thus an assumption about the long-range ($Q^2 \lesssim 1\,\text{GeV}^2$) behaviour of the interaction. Requiring that Ward-Takahashi identities be automatically fulfilled by any truncation entails [9,11] that the kernel in the renormalised gap equation is expressed through

$$\mathcal{G}(Q^2)\, D^{\text{free}}_{\mu\nu}(Q)\frac{\lambda^a}{2}\gamma_\mu S(q)\frac{\lambda^a}{2}\gamma_\nu\,, \tag{8}$$

where we have introduced $\mathcal{G}(Q^2)$, an effective interaction, to emphasise that, while $\mathcal{G}(Q^2) = 4\pi\alpha(Q^2)$ is well determined for $Q^2 \gtrsim 1\,\text{GeV}^2$, the behaviour at $Q^2 < 1\,\text{GeV}^2$, *i.e.*, at infrared length-scales ($\gtrsim 0.2\,\text{fm}$), of the kernels in the gap and Bethe-Salpeter equations is unknown.

Contemporary DSE studies employ a model for the infrared behaviour. The most extensively applied is [3]

$$\begin{aligned} \frac{\mathcal{G}(Q^2)}{Q^2} &= \frac{4\pi^2}{\omega^6} D\, Q^2 \mathrm{e}^{-Q^2/\omega^2} \\ &\quad + 8\pi\, \frac{\pi\,\gamma_m}{\ln\left[\tau + \left(1 + Q^2/\Lambda^2_{\text{QCD}}\right)^2\right]}\, \mathcal{F}(Q^2)\,, \end{aligned} \tag{9}$$

Table 2. Calculated pion decay constant and vacuum quark condensate. Experimentally, $f_\pi = 0.092$, and a best phenomenological value of the condensate is $-\langle\bar{q}q\rangle^0_{1\,\text{GeV}} = (0.236 \pm 0.008)^3$ [13]. (All quantities are listed in GeV.)

Model	f_π	$(-\langle\bar{q}q\rangle^0_{1\,\text{GeV}})^{1/3}$
eqs. (9), (10)	0.092	0.24
eqs. (14), (15)	0.053	0.15
eqs. (14), (16)	0.099	0.25

where $\mathcal{F}(Q^2) = [1 - \exp(-k^2/[4m_t^2])]/k^2$, $m_t = 0.5\,\text{GeV}$, $\tau = \mathrm{e}^2 - 1$, $\gamma_m = 12/(33 - 2N_f)$, $N_f = 4$, and $\Lambda_{\text{QCD}} = \Lambda^{(4)}_{\overline{\text{MS}}} = 0.234\,\text{GeV}$ [14] (N.B. eq. (9) gives $\alpha(m_Z^2) = 0.126$. Comparison with a modern value [15], $0.113^{+0.009}_{-0.013}$, means that a smaller Λ_{QCD} is acceptable in the model, if one wants to avoid overestimating the coupling in the ultraviolet, but not a larger value.) The true parameters in eq. (9) are D and ω, which together determine the interaction tension in the model. However, they are not independent: in fitting, a change in one is compensated by altering the other; *e.g.*, on the domain $\omega \in [0.3, 0.5]\,\text{GeV}$, the fitted observables are approximately constant along the trajectory $\omega\, D = (0.72\,\text{GeV})^3$. This correlation, a reduction in D compensating for an increase in ω, acts to keep a fixed value of the interaction tension; *i.e.*, the interaction's integrated strength on the infrared domain. With

$$D = (0.96\,\text{GeV})^2\,,\ \omega = 0.4\,\text{GeV} \tag{10}$$

and current-quark masses

$$m_u^{1\,\text{GeV}} = 5.5\,\text{MeV}\,,\ m_s^{1\,\text{GeV}} = 125\,\text{MeV}\,, \tag{11}$$

one obtains the excellent description of meson observables described in the introduction, which can be illustrated via the calculated values of the leptonic decay constant and vacuum quark condensate in table 2.

2.3 Comparison with lattice-QCD simulations

The scalar functions characterising the renormalised dressed-quark propagator, *i.e.* the wave function renormalisation, $Z(p^2)$, and the mass function, $M(p^2)$, obtained by solving the renormalised gap equation using eq. (9), are depicted in figs. 2, 3. The infrared suppression of $Z(p^2)$ and enhancement of $M(p^2)$ are long-standing predictions of DSE studies, as ref. [16] makes plain and could be anticipated from ref. [17]. This prediction has recently been confirmed in numerical simulations of quenched lattice-QCD, as is evident in the figures.

It is not yet possible to reliably determine the chiral limit behaviour of lattice Schwinger functions. Hence one does not have a lattice estimate for the quantities in table 2. To obtain such an estimate, we used the DSE model described previously, varying (D, ω) in order to reproduce the lattice data. Our current best result, obtained with

$$D = (0.74\,\text{GeV})^2\,,\ \omega = 0.3\,\text{GeV}\,, \tag{12}$$

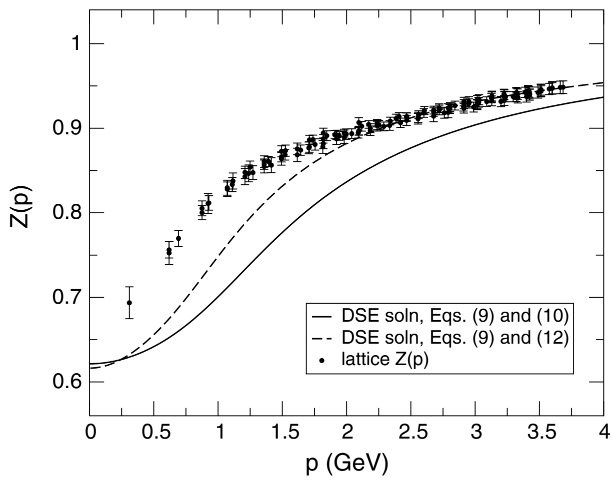

Fig. 2. Wave function renormalisation. Solid line: solution of the renormalised gap equation using eqs. (9), (10); data: lattice simulations [18], $m = 0.036/a \sim 60\,\mathrm{MeV}$; dashed line: gap equation solution using eqs. (9), (12). (In the DSE studies, the renormalisation point $\zeta = 19\,\mathrm{GeV}$ and the current-quark mass is $0.6\, m_s^{1\,\mathrm{GeV}}$ (eq. (11)).)

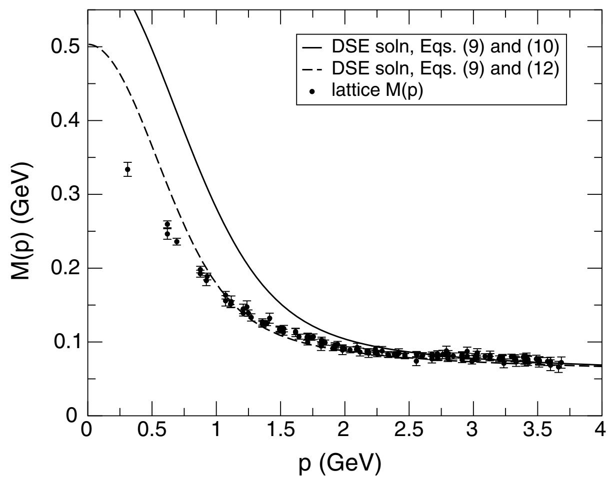

Fig. 3. Mass function. Solid line: solution of the renormalised gap equation using using eqs. (9), (10); data: lattice simulations [18], $m = 0.036/a \sim 60\,\mathrm{MeV}$; dashed line: gap equation solution using eqs. (9), (12). (In the DSE studies, the renormalisation point $\zeta = 19\,\mathrm{GeV}$ and the current-quark mass is $0.6\, m_s^{1\,\mathrm{GeV}}$ (eq. (11)).)

at a current-quark mass of $0.6\, m_s^{1\,\mathrm{GeV}}$, eq. (11), is also depicted in figs. 2, 3, and yields $f_\pi = 0.094\,\mathrm{GeV}$, $m_\pi = 0.48\,\mathrm{GeV}$. (N.B. These are values for a pion-like bound state constructed from constituents whose current-quark mass is $m \approx 14\, m_u$. Our DSE-calculated meson mass *versus* current-quark mass trajectory is consistent with results of recent quenched lattice-QCD simulations obtained on $m \in [1,2]\, m_s$ [10].) The parameters in eq. (12) give chiral limit results:

$$f_\pi^0 = 0.068\,\mathrm{GeV}\,,\ -\langle \bar{q}q\rangle^0_{1\,\mathrm{GeV}} = (0.19\,\mathrm{GeV})^3\,. \qquad (13)$$

2.4 Gap equation and QCD's gauge sector

Contemporary Landau gauge DSE studies of QCD's gauge sector have been used to infer a form of the effective interaction [19], which is well represented by ($x = Q^2/\Lambda^2_{\mathrm{QCD}}$)

$$\frac{1}{4\pi}\mathcal{G}(x) := \alpha(x) = \frac{a_0 + a_1 x}{1 + a_2 x + a_3 x^2 + a_4 x^3} + \frac{\pi\,\gamma_m}{\ln(e+x)}\,, \qquad (14)$$

$$\frac{a_0 \quad a_1 \quad a_2 \quad a_3 \quad a_4}{1.47 \quad 0.881 \quad 0.314 \quad 0.00986 \quad 0.00168}\,. \qquad (15)$$

Aspects of these DSE studies are in qualitative agreement with quenched lattice-QCD results [20]; *e.g.*, the feature that the dressed-gluon propagator is finite at $Q^2 = 0$. This effective interaction yields the results in the second row of table 2: apparently, f_π is too small by a factor of ~ 2 and the scale of DCSB too small by a factor of $\sim 4 = 1.6^3$ [21]. This outcome could have been anticipated from ref. [7].

Equations (7), (8) are correct on the ultraviolet domain in which perturbation theory is applicable. However, modelling is involved in extrapolating onto the infrared domain. One may require that multiplicative renormalisability of the dressed fermion propagator be preserved in this modelling [22]. The *Ansatz* of ref. [23] incorporates this constraint; however, it implicitly specifies a kernel in the gap equation that violates a more important constraint, namely, Lorentz covariance [24]. A minimal *Ansatz* that satisfies both constraints and eq. (7) finds expression in the kernel of the renormalised gap equation as

$$4\pi\alpha(Q^2)\frac{1}{Z^2(Q^2)}\, D_{\mu\nu}^{\mathrm{free}}(Q)\frac{\lambda^a}{2}\gamma_\mu S(q)\frac{\lambda^a}{2}\gamma_\nu\,. \qquad (16)$$

The gap equation's solution now gives the results in the third row of table 2. (We simplified the numerical study by using a well-tried angle approximation: $\alpha((k-q)^2)/Z^2((k-q)^2) \approx \alpha((k-q)^2)/Z^2(\max(k^2,q^2))$.) This procedure is evidently a candidate for providing a bridge between DSE studies of the gauge sector and what is known, from the calculation of observables, to be the infrared strength required in the effective interaction. The increased interaction tension arises because the enhancement of $1/Z(p^2)$, evident in fig. 2, persists with this kernel and amplifies the effective coupling: the interaction tension calculated with eq. (14) alone is $\sigma^\Delta = 12\,\mathrm{GeV/fm}$, but using eq. (16) we estimate that the $1/Z^2(Q^2)$ factor raises this to $\sigma^\Delta \sim 25\,\mathrm{GeV/fm}$.

3 Confinement

This is a statement about the properties of coloured Schwinger functions; *i.e.*, gauge-dependent quantities. Hence it is plausible that the expression of confinement will depend on the gauge-fixing procedure one employs. Linear covariant gauges are most widely employed in DSE studies. While the problem of Gribov copies is unresolved, it affects only the far infrared behaviour of coloured Schwinger functions and hence is hoped to have little impact on physical observables. This conjecture is supported by the close correspondence between Landau and Laplacian gauge two-point quark and gluon Schwinger functions obtained in quenched lattice-QCD simulations [25]. (Laplacian gauge fixing is a nonlocal prescription that is identical to Landau gauge at ultraviolet momenta. It is free of Gribov copies.)

It has long been known [26] that for confinement it is sufficient that no coloured Schwinger function possess a spectral representation. This is equivalent to the statement that all coloured Schwinger functions violate reflection positivity. That property can manifest itself *almost* as simply as, say, dressed-gluons being described by a propagator with a large width. The connection between confinement and the violation of reflection positivity has cleanly been illustrated in QED3 [27], and it is a result of DSE studies that a sufficiently large interaction tension will always produce a dressed-quark propagator that violates reflection positivity. (N.B. Gap equation solutions that violate reflection positivity also exhibit DCSB. The converse is not necessarily true.) Thus, it is a widespread conjecture that confinement in QCD is realised this way.

A Schwinger function that violates reflection positivity is easily identified: it is sufficient that the function exhibit a maximum or inflection at some spacelike four-momentum-squared. In lattice-QCD simulations, this feature is evident in the two-point gluon Schwinger function [20] and incipient in the scalar functions characterising the dressed-quark two-point function [18]. It is plain in our results for the dressed-quark propagator, figs. 2, 3, and apparent in the DSE result for the gluon two-point function [28]. The DSE solution for the ghost two-point function also violates reflection positivity but in this case it is manifest in the strength of its singularity at $k^2 = 0$.

A consistent picture may be emerging. It is complemented by the fact that the colour-singlet S-matrix elements which describe physical processes do not exhibit unphysical quark and gluon production thresholds when calculated using coloured Schwinger functions that violate reflection positivity. The ideas we have described also ensure that coloured composites such as diquarks do not appear in the spectrum [9,11].

4 Epilogue

The momentum-dependent dressing of quark and gluon propagators is a fact. It is certainly the keystone of DCSB and quite likely plays a central role in confinement. Its incorporation into models of low-energy phenomena facilitates the development of a qualitatively reliable understanding and makes possible an excellent description of experiment. That has provided guidance for modelling the long-range behaviour of the interaction between light-quarks. A remaining challenge is to calculate it and progress is being made.

We thank P.O. Bowman for the lattice data and P.C. Tandy for a careful reading of the manuscript. PM and AR are grateful for the hospitality and support of the Physics Division at ANL during visits in which part of this work was conducted. This work was supported by the Deutsche Forschungsgemeinschaft, contract no. Ro 1146/3-1; the US Department of Energy (DOE), Nuclear Physics Division, contract no. W-31-109-ENG-38; DOE grant nos. DE-FG02-96-ER-40947, DE-FG02-97-ER-41048; and benefited from the resources of the US National Energy Research Scientific Computing Center.

References

1. C.D. Roberts, S.M. Schmidt, Prog. Part. Nucl. Phys. **45**, S1 (2000); R. Alkofer, L. v. Smekal, Phys. Rep. **353**, 281 (2001).
2. P. Maris, C.D. Roberts, Phys. Rev. C **56**, 3369 (1997).
3. P. Maris, P.C. Tandy, Phys. Rev. C **60**, 055214 (1999).
4. P. Bicudo, *et al.*, Phys. Rev. D **65**, 076008 (2002); D. Jarecke, P. Maris, P.C. Tandy, *Strong decays of light vector mesons*, nucl-th/0208019.
5. P. Maris, P.C. Tandy, Phys. Rev. C **62**, 055204 (2000); C.R. Ji, P. Maris, Phys. Rev. D **64**, 014032 (2001); P. Maris, P.C. Tandy, Phys. Rev. C **65**, 045211 (2002).
6. P. Maris, C.D. Roberts, P.C. Tandy, Phys. Lett. B **420**, 267 (1998).
7. F.T. Hawes, P. Maris, C.D. Roberts, Phys. Lett. B **440**, 353 (1998).
8. C.D. Roberts, *Continuum strong QCD: Confinement and dynamical chiral symmetry breaking*, nucl-th/0007054.
9. A. Bender, C.D. Roberts, L. v. Smekal, Phys. Lett. B **380**, 7 (1996).
10. C.D. Roberts, Nucl. Phys. Proc. Suppl. **108**, 227 (2002).
11. A. Bender, W. Detmold, A.W. Thomas, C.D. Roberts, Phys. Rev. C **65**, 065203 (2002).
12. H.J. Munczek, A.M. Nemirovsky, Phys. Rev. D **28**, 181 (1983).
13. D.B. Leinweber, Ann. Phys. (N.Y.) **254**, 328 (1997).
14. Particle Data Group Collaboration (L. Montanet *et al.*), Phys. Rev. D **50**, 1173 (1994).
15. Particle Data Group Collaboration (D.E. Groom *et al.*), Eur. Phys. J. C **15**, 1 (2000).
16. C.D. Roberts, A.G. Williams, Prog. Part. Nucl. Phys. **33**, 477 (1994).
17. K. Johnson, M. Baker, R. Willey, Phys. Rev. **136**, B1111 (1964).
18. P.O. Bowman, U.M. Heller, A.G. Williams, Phys. Rev. D **66**, 014505 (2002).
19. R. Alkofer, C.S. Fischer, L. v. Smekal, Acta Phys. Slov. **52**, 191 (2002) and references therein.
20. F.D. Bonnet, *et al.*, Phys. Rev. D **64**, 034501 (2001).
21. These results are in agreement with M. Bhagwat, M.A. Pichowsky, P.C. Tandy, private communication.
22. D.C. Curtis, M.R. Pennington, Phys. Rev. D **42**, 4165 (1990).
23. J.C.R. Bloch, *Multiplicative renormalizability and quark propagator*, hep-ph/0202073.
24. C.J. Burden, C.D. Roberts, Phys. Rev. D **47**, 5581 (1993).
25. P.O. Bowman, U.M. Heller, A.G. Williams, Nucl. Phys. Proc. Suppl. **109**, 163 (2002); P.O. Bowman, U.M. Heller, D.B. Leinweber, A.G. Williams, *Gluon propagator on coarse lattices in Laplacian gauges*, hep-lat/0206010.
26. G. Krein, C.D. Roberts, A.G. Williams, Int. J. Mod. Phys. A **7**, 5607 (1992).
27. P. Maris, Phys. Rev. D **52**, 6087 (1995).
28. R. Alkofer, L. v. Smekal, Nucl. Phys. A **680**, 133 (2000).